ELSEVIER

Marine Chemistry 70 (2000) 339–357

MARINE CHEMISTRY

www.elsevier.nl/locate/marchem

The relationship between chromophoric dissolved organic matter and dissolved organic carbon in the European Atlantic coastal area and in the West Mediterranean Sea (Gulf of Lions)

Giovanni M. Ferrari *

Joint Research Centre, Space Applications Institute, C.E.C., Ispra Site, 21020 Ispra (VA), Italy

Received 19 May 1999; accepted 10 February 2000

Abstract

The absorption coefficient of chromophoric dissolved organic matter (aCDOM) has been found to be correlated with fluorescence emission (excitation at 355 nm). In the coastal European Atlantic area and in the Western Mediterranean Sea (Gulf of Lions), a significant statistical dependence has been found between aCDOM and fluorescence with dissolved organic carbon (DOC) concentration. The relationship shows that, in the river plume areas (Rhine in the North Sea and Rhône in the Gulf of Lions), a consistent fraction of DOC (from 40% to 60% of the average of the DOC measured) is non-absorbing in visible light range, where the dissolved organic matter (DOM) is typically absorbent. In comparison, in the open sea, apparently not affected by the continental inputs, the entire DOC belongs to the chromophoric DOM whose specific absorption is lower (5 to 10 times) than that found in the river plume areas.

Keywords: chromophoric dissolved organic matter; dissolved organic carbon; European Atlantic coastal area; West Mediterranean Sea (Gulf of Lions)

1. Introduction

Dissolved organic matter (DOM) is recognised as having an important role in the photo-chemistry of the organic material in surface waters. The UV-induced photo-transients of DOM produce photochemical degradation of materials not photo-chemically altered otherwise (Zepp et al., 1977; Helz et al., 1994). A further active role of marine DOM and its associated parameter dissolved organic carbon (DOC) has been recognised in the photochemical degradation of dimetylsulfide (DMS) (Brugger et al., 1998). In this context of generalised interest, the quantification as well as the understanding of the origin and the fate of DOM in the coastal areas and in the open sea, need to be improved. Moreover, DOM is the most important sunlight-absorbing substance in the

* Tel.: +39-332-789-111; fax: +39-332-789-034.
E-mail address: massimo.ferrari@jrc.it (G.M. Ferrari).

0304-4203/00/$ - see front matter
PII: S0304-4203(00)00036-0

sea especially in the UV and blue regions of the spectrum (Højerslev, 1988). In the coastal areas of the southern Baltic Sea, DOM absorption alone can reach up to three times the absorption of particulate matter in pure water in the wavelength range of 400–500 nm (Ferrari and Dowell, 1998). Chromophoric dissolved organic matter (CDOM) represents the fraction of DOM absorbing visible light. Its optical properties provide information on DOM as a whole and on DOC which are the fundamental parameters for organic matter and carbon flux studies in aquatic ecosystems (Bacastow and Maier-Reimer, 1991; Jackson, 1993). At present, knowledge on CDOM, DOM and DOC relationships is insufficient because only few, although significant, works have been specifically addressed to this subject (Vodacek et al., 1995, 1997, Nieke et al., 1997, Chen, 1999). Optical properties of CDOM such as absorption and fluorescence are currently used in passive Remote Sensing (RS) techniques to correct the retrieved chlorophyll concentration and, in some cases, to retrieve CDOM absorption (aCDOM) when chlorophyll concentration is negligible (Hoge et al., 1995a). Another useful property of CDOM is the UV light-induced fluorescence which is generally well correlated with CDOM absorption (Ferrari and Tassan, 1991; Hoge et al., 1993; Green and Blough, 1994). This relationship allows an application of active Remote Sensing using an airborne Lidar technique to infer CDOM absorption over large areas in real time measuring the incoming laser induced fluorescence (Hoge et al., 1995a,b). CDOM absorption as well as the induced fluorescence can represent a useful parameter to trace DOC concentration when a correlation is established. A significant correlation between aCDOM or fluorescence and the total DOC has been found strictly linked to the space-temporal homogeneity of the area investigated in coastal zones (Ferrari et al., 1996; Vodacek et al., 1997).

The aim of this work is to contribute to the knowledge of CDOM absorption, CDOM fluorescence and DOC inter-relationship in the coastal areas of the sea. The sites investigated were the European Atlantic coastal area and adjacent seas influenced by the rivers Rhine (North Sea) and Rhône (Gulf of Lions, West-Mediterranean Sea). The data, acquired in the limits of the maximum possible accuracy, can contribute to enrich the data bank for RS algorithms and optical models development. Furthermore, they can be used for DOM/DOC flux studies addressed to evaluate the influence of the coastal zones on the open ocean. Here all the results presented are obtained during two cruises: in the Atlantic area (April 1997) and in the Gulf of Lions (September–October 1997). The cruises were organised within the framework of the CoastLooc project (1996–1999) funded by the European Commission.

2. Methods

2.1. Study sites and sample collection

The European Atlantic coast was the first investigation area selected because of its oceanographic characteristics determined by the spatial variability of the bio-geo-optical parameters. This variability, overall in low values, provided an effective test for the applied ''in situ'' methodology both for the instrumental measurements (optical profilers) and for the discrete ones (water samples). A cruise was planned by the universities of Bremen and Oldenburg (Germany) in the frame of the CoastLooc project and performed in April 1997 with the oceanographic R/V *Victor Hensen* (Reedereigemeinschaft Forschungsschiffahrt, Bremen). The survey covered an extended area from the German Bight (North Sea) to the Canary Islands (Spain) as illustrated in Fig. 1. The investigation strategy was addressed (1) to intensively sample the turbid and the plankton-rich waters of the Rhine river plume in the North Sea (Stations 1 to 9) and (2) to sample in the continental shelf (Stations 10 to 12), in the canyons of the continental slope (Stations 12 to 15). Furthermore, some samples have been collected in the coastal–oceanic banks as well as in area of the flat summit of the sea mounts (Stations from the Brittany banks to the Bank of Amanay in the Canary islands). The second area investigated was the Gulf of Lions in the West Mediterranean Sea. Also in this case, the sampling objective was to investigate the Case 2 waters where, CDOM, total particulate matter and chlorophyll are not inter-correlated, and where the influence of the continental inputs (from the Rhône river) as fresh waters, suspended and dissolved materials

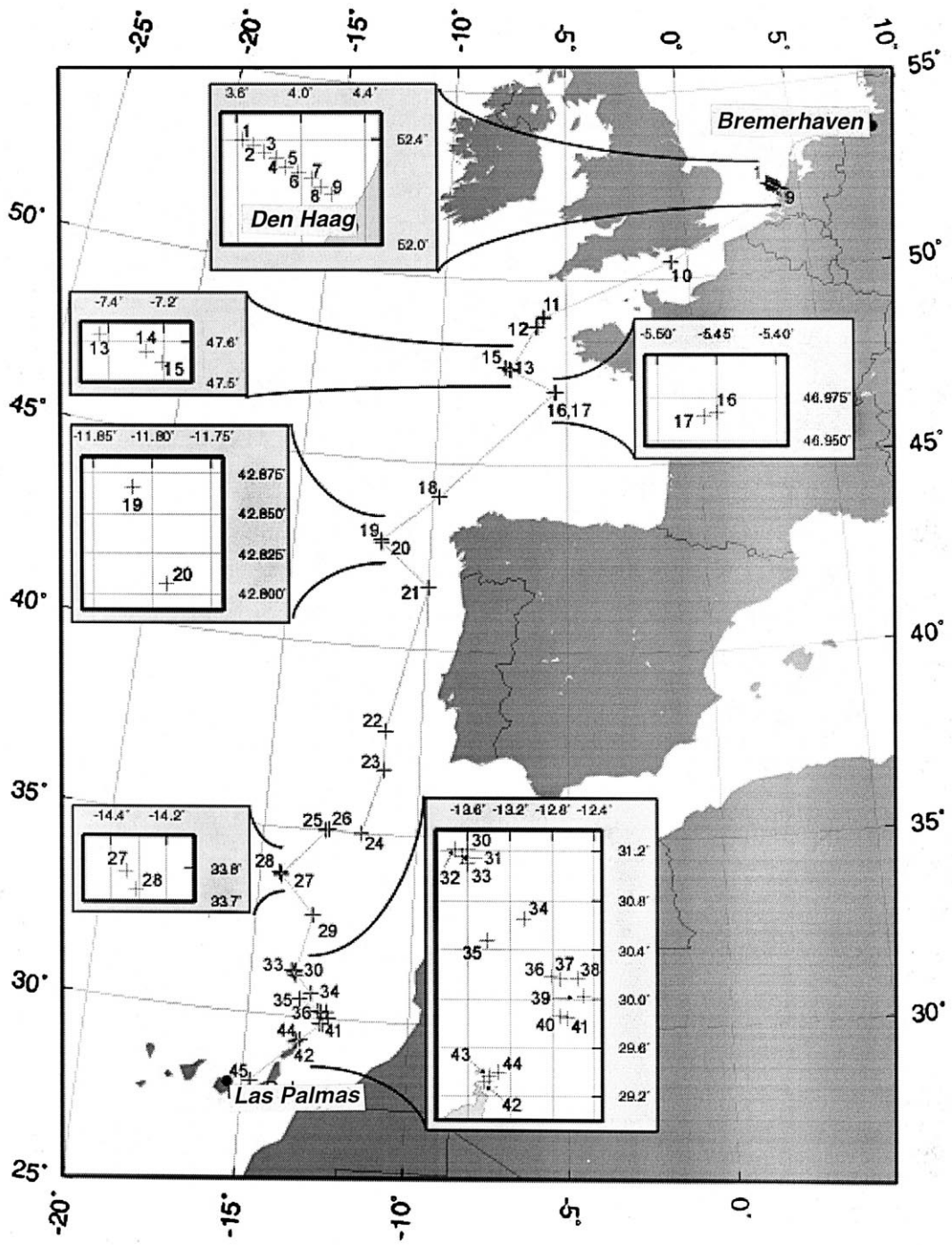

Fig. 1. Map showing the location of the stations visited during the *Victor Hensen* cruise in the North Sea and in the European coastal Atlantic areas (04/02/97–04/22/97).

are predominant in the marine environment considered. After the construction of the Aswan dam, which has drastically reduced the input of the Nile river, the Rhône became the biggest river flowing into the Mediterranean Sea (Gulf of Lions) with a mean discharge = 1750 m^3 s^{-1} (Naudin et al., 1997). The sampling grid has been designed to encompass the large gradient of the geophysical parameters determined by the Rhône river waters in the basin considered (Fig. 2). The main fraction of the samples was collected on the continental shelf where, in the season considered, the water body is characterised by a strong and a time–space variable stratification. The cruise was organised and conducted by the Coast-Looc project team during the period from 09/28/97 to 10/09/97 using the R/V *Thetys* of the INSU (France).

2.2. Sample collection

During these cruises, particular attention has been dedicated to water sample preparation in order to reduce, as much as possible, the time from the water collection until the measurement or laboratory analysis. The basic criterion was to collect surface samples with a bucket, and with Niskin bottles, at the

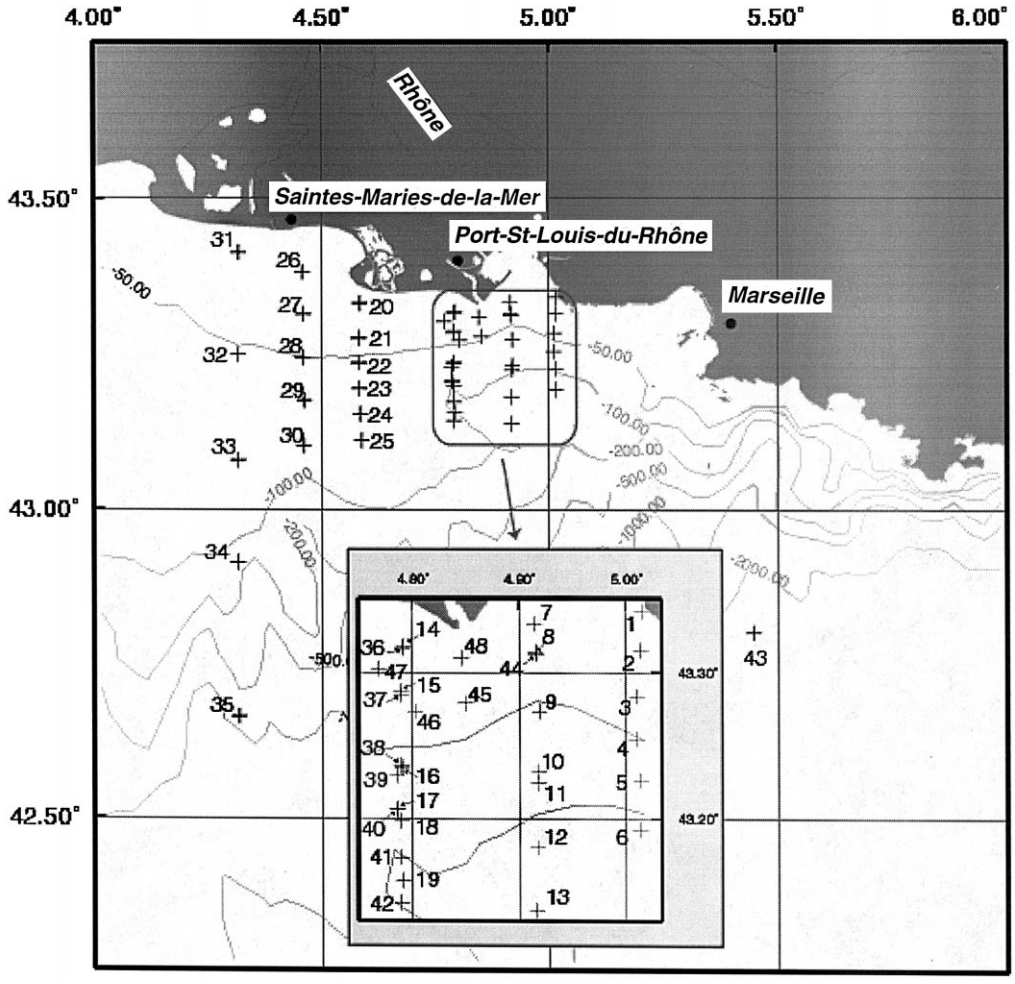

Fig. 2. Map showing the location of the stations visited during the *Thetys* cruise in the Gulf of Lions (09/28/97–10/09/97).

chlorophyll maximum depth and, sometimes, under the chlorophyll maximum depth. The bio-optical structure of the water body was determined using a multi-parametric profiler, home made at the University of Oldenburg (Germany). The instrument included a CTD type Meerestechnik Elektronic OTS 1500, which acquired temperature and salinity, and a multichannel fluorometer (three excitation channels such as: 420 and 530 nm for the detection of chlorophyll and 270 nm for CDOM) (Heuermann et al., 1995). The profiler was a prototype polychromatic daylight radiometer for measurement of upwelling and downwelling irradiance between 340 and 760 nm (one value each 2.5 nm). For the discrete sampling, the water was immediately filtered with a 0.22 μm Millipore membrane previously rinsed with 50 ml of Milli-Q water under a slight vacuum of 650 mm Hg. At the same time, a series of duplicate samples were obtained with gravity filtration ($h = 10$ cm) using Whatman GFF glass-fibre filters.

3. Absorption and fluorescence measurements of CDOM

3.1. Absorption measurements

A fraction of filtered water was immediately measured as absorption with a Perkin-Elmer Lambda 12 double beam spectrophotometer installed on board. The spectra were acquired in the range 350–750 nm with the reference, a quartz cuvette filled with MilliQ water, automatically subtracted. Particular attention was given to the cleaning of the cuvettes and to the temperature of the sample and the reference. A specific study has demonstrated that a difference of temperature of 2°C to 12°C can introduce artefacts in the spectrum with a more or less prominent negative peak at 735 nm. The temperature tends to increase in the measurement compartment and in the reference cuvette, with respect to that of the sample that is generally colder. Furthermore, inadequate MilliQ water cleaning and rinsing of the cuvettes can produce a shift of the spectrum due probably to the light backscattered by the thin film of salts on the quartz surface. The high probability to encounter these errors especially, operating ''in situ'' has suggested the option to consider the absorbance value at 650 nm as zero and consequently correct all the spectra. This assumption is sufficiently supported by the following two reasons.

(a) The molecular nature of the organic chromophores of the CDOM allows the CDOM scattering to be considered equal to the Rayleigh scattering of the pure water, thus implying that CDOM scattering itself can be neglected.

(b) CDOM absorption coefficient (aCDOM, expressed in m^{-1}) is derived by the transformation of the absorbance (ACDOM, dimensionless) using the: $aCDOM = ACDOM \times 2.3/L$, where L is the optical pathway in meters. It is generally accepted that aCDOM follows with the wavelength a roughly exponential law as modelled by Bricaud et al. (1981)

$$aCDOM(\lambda) = aCDOM(\lambda_0)\exp\{-S(\lambda - \lambda_0)\} \quad (1)$$

where S is the slope of the semi-logarithmic expression and it is dependent on the light reactivity of the chromophores of the different types of DOM. Generally, S is low in the coastal areas in proximity of the continental inputs (0.013–0.018) and higher in the open ocean (up to 0.025 and more). If the lower S is applied, even considering the maximum values obtained during the cruises here described, the absorption obtained at 650 nm was found lower than the instrumental photometric accuracy, which is given as 0.003 absorbance units.

Due to the chemical composite nature of CDOM in natural waters, it is practically impossible to use light absorption to identify a particular group of chromophores as well as, obviously, a single chromophore. S is calculated by linear fitting to the semi-logarithmic plot from 350 to 480 nm. This encompasses all the measurable values. This range has been chosen to avoid introducing in the fit, values affected by a low signal to noise ratio and by edges or anomalous curvatures occurring sometimes in the low region of the spectrum which can strongly alter the fit. Generally, S depends, in some degree, on the wavelength range chosen. In the Baltic Sea (Ferrari and Dowell, 1998), the difference between two slopes measured in the range: 355–420 nm and 400–600 nm, was in the order of 4.13% ± 2.3% for

14 groups of observations. Furthermore, S does not behave as a conservative parameter when mixing different water masses. In fact, mixing of waters with a distinct S, the resulting Si gives a spectrum exhibiting a multi-exponential decay as (Green, 1992)

$$a(\lambda) = \sum_{1}^{n} ai(\lambda_0)\exp\{-Si(\lambda - \lambda_0)\} \quad (2)$$

which gives a continuous curve when $\ln(a)$ is plotted vs. λ. In practice, this expression suggests that, even when n is small, it is almost impossible to distinguish the different S forming the composite curve with slope Si. In other words, the seldom-observed non-linear plots of the semi-log curve cannot be used to derive the composition of or the sources of the CDOM present in the water masses.

The ensembles of the data useful for this article relative to the *Victor Hensen* and the *Thetys* cruises are given in Appendices A and B, respectively.

3.2. Fluorescence and quantum yield measurement

As for the absorption, fluorescence was immediately measured after the sample collection and filtration. In this way, we avoid all the controversial and unresolved problems linked to the sample preservation. The spectro-fluorimeter used was the Perkin-Elmer LS50 operating in emission mode. All the details regarding the operational conditions are given in Ferrari et al. (1996) and Ferrari and Dowell (1998). The fluorescence emission unit obtained in this work is the standardised fluorescence unit (St.F.U.):

$$F_s/F_{qs} \times 10 = \text{St.F.U.}(\lambda) \quad (3)$$

where F_s is the fluorescence measured as emission peak height (at 430–450 nm), F_{qs} is the fluorescence of a standard solution of quinine sulphate (0.01 mg/l in 1 N H_2SO_4), λ is the excitation wavelength at 355 nm. MilliQ water was used as a blank and its fluorescence subtracted by each sample measurements, while a solution of 1 N H_2SO_4 was used as a blank to obtain quinine sulphate measurement. Quinine sulphate is employed here as an external standard to account for each instrumental drift, especially for the xenon pulsed lamp time decay. The quinine sulphate was measured twice per day and used in the Eq. 3. Given the relatively low values of CDOM absorption, no correction has been made for the inner filter effect as described in Ferrari and Tassan (1991).

Quantum yield has been calculated on the basis of the fluorescence emission with excitation light at 355 nm and the absorption coefficient at 355 nm. A quinine sulphate, 0.5 mg/l in 0.1 N H_2SO_4 was used as reference. The expression was the following (Green, 1992):

$$\Phi_s(\lambda) = \{F_s \times a_r \times \Phi_r\}/\{a_s \times F_r\} \quad (4)$$

where subscripts s and r refer to the sample and reference respectively, a is the absorption coefficient of each at its excitation wavelength (355 nm), F is the fluorescence intensity integrated between 420 and 460 nm and Φ_r is the quantum yield of quinine sulphate, 0.55.

4. DOC measurement

In order to reduce the sources of contamination, particular care has been dedicated to the DOC sample preparation. Amber-glass bottles (100 ml) were treated with 20% HCl for 12 h, rinsed with MilliQ water and placed in a muffle furnace at 120°C for 12 h. After cooling, the bottles were closed with acid cleaned Nylon caps. Water samples were stored in a 15-l seawater preconditioned polypropylene container and from this, filtered on a 0.22 μm Millipore membrane pre-rinsed with Milli-Q water, using a slight depression of 200 mm Hg. In each filtration the initial aliquot (200 ml) was discarded to prevent the possible source of contamination by the filters. The final filtrate was transferred to the bottle pre-rinsed with the same filtered seawater and acidified with 0.5 ml of 50% H_3PO_4 and stored in refrigerator at 2–4°C as recommended by the JGOFS protocol. The samples have been analysed within 3 weeks at JRC Ispra Environment Institute.

4.1. HTCO method

A Carlo Erba 480 analyser was used for DOC determination with high temperature catalytic oxidation (HTCO). All the details regarding the instrumental methodology as well as the analytical error esti-

mate can be found in Ferrari et al. (1996). With respect to the description given in the reference cited, we have changed the automatic sample valve, which now injects 100 μl instead of the previous 50 μl, to increase the basic signal to noise ratio. This new valve has possibly contributed to lower the instrumental blank for Milli-Q water (Millipore, Super Q Water System) to 50 μMC (45,000 counts, ±5% on 15 observations). We have tried to assess which portion of the instrumental blank is due to the residual carbon in Milli-Q water with respect to that due to the catalyst as well as the hydrogen and the nitrogen used as purging and carrier gas. The operation was made with the peristaltic pump closed, thus omitting the injection of liquid into the circuits; however, the pressure was maintained equivalent through the injection of additional purging gas. The result (20 μMC, 18,600 counts, ±1.9% on 10 observations) indicates that the main portion of the blank is due to the water injection (30 μMC) and not to the carrier gases. In addition to the description given in the reference, we also note here that the ceramic reactor was filled with NiO in alternate layers with quartz wool. This accounts for any possibility that the instrumental plant can be strongly affected by the catalyst in case of use of other supports instead of quartz (e.g. alumina, Cauwet, 1994). At the moment of the revision of this article, using truly carbon-free water, the blank level is reduced to less than 25 μMC. However, at the time of the sample measurements, the estimated blank accuracy was stable: ±5% for 40 observations. The analytical precision was calculated to be on the order of 2% and it falls in the range of the recent upgraded HTCO method (Sharp et al., 1995; Sharp, 1997). The DOC data of the two cruises described in this work can be found in the Appendices A and B.

5. Results and discussion

During these cruises, the use of different filters for the acquisition of the CDOM absorbance spectra was evaluated. We have compared the filtrates obtained by gravity filtration (without depression) on Whatman GFF glass-fibre filters against the filtrates from the 0.22 μm Millipore membrane under gentle filtration (650 mm Hg). The aim was to check the presence of a consistent fraction of DOM, the size of which can be included in the range of 0.7 μm (the average porosity of Whatman GFF filter) to 0.22 μm (the porosity of cellulose Millipore filter). Actually, the 0.22 μm pore size is assumed as the conventional limit to separate dissolved from particulate matter but, on the other hand, the GFF filter is widely used for several oceanographic/optical measurements on the total suspended matter (TSM) such as: dry weight, CHN analysis, in-vivo absorption of pigment and detritus. The results have shown a difference (on average) aCDOM(from GFF) − aCDOM (from Millipore 0.22 μm): +6.6%(±29) for the samples collected at depth in the Atlantic areas and +7.4% (±16) for the surface samples only. The differences are much lower in the Mediterranean area (Gulf of Lions): +1.4%(±9.5). Excluding other sources of error (the instrument, the measurement range and the operator were the same), we can conclude that the differences found, considering also the variability due to some outlying values, especially for the low values of the Atlantic area, are not so large, thus justifying the use of GFF filters for the purposes described below. Semi-logarithmic plots of absorption spectra of CDOM of fluvial origin were compared in magnitude and slope with those of the open sea areas. The differences in slopes are not as outstanding as the differences in magnitude, although the aCDOM slopes S of the open sea areas are undoubtedly steeper than those of estuarine areas (data in Appendices A and B). The spectral slope S of Eq. 1 was acquired by fitting the absorbance data (from 350 and 480 nm) and only considering the values greater than 0.003, which is the photometric instrumental accuracy. If we analyse the data given in Appendices A and B we find that, for the Atlantic cruise (VH), S is on average 0.0185(±0.005) in surface, 0.0163 (±0.003) at the euphotic depth, and 0.0133(±0.003) below the euphotic depth. In the Mediterranean area, as illustrated in Fig. 2, the samples were collected mainly on the continental shelf between the isobath at less than 50 m and that of 200 m in the Gulf of Lions. CTD profiles (H. Barth, unpublished data) exhibit a thermocline with a sharp temperature gradient between 22.7°C in surface and in the stratified upper layer, and 14–14.5°C in the deep waters. Fig. 3 illustrates, as an example for the

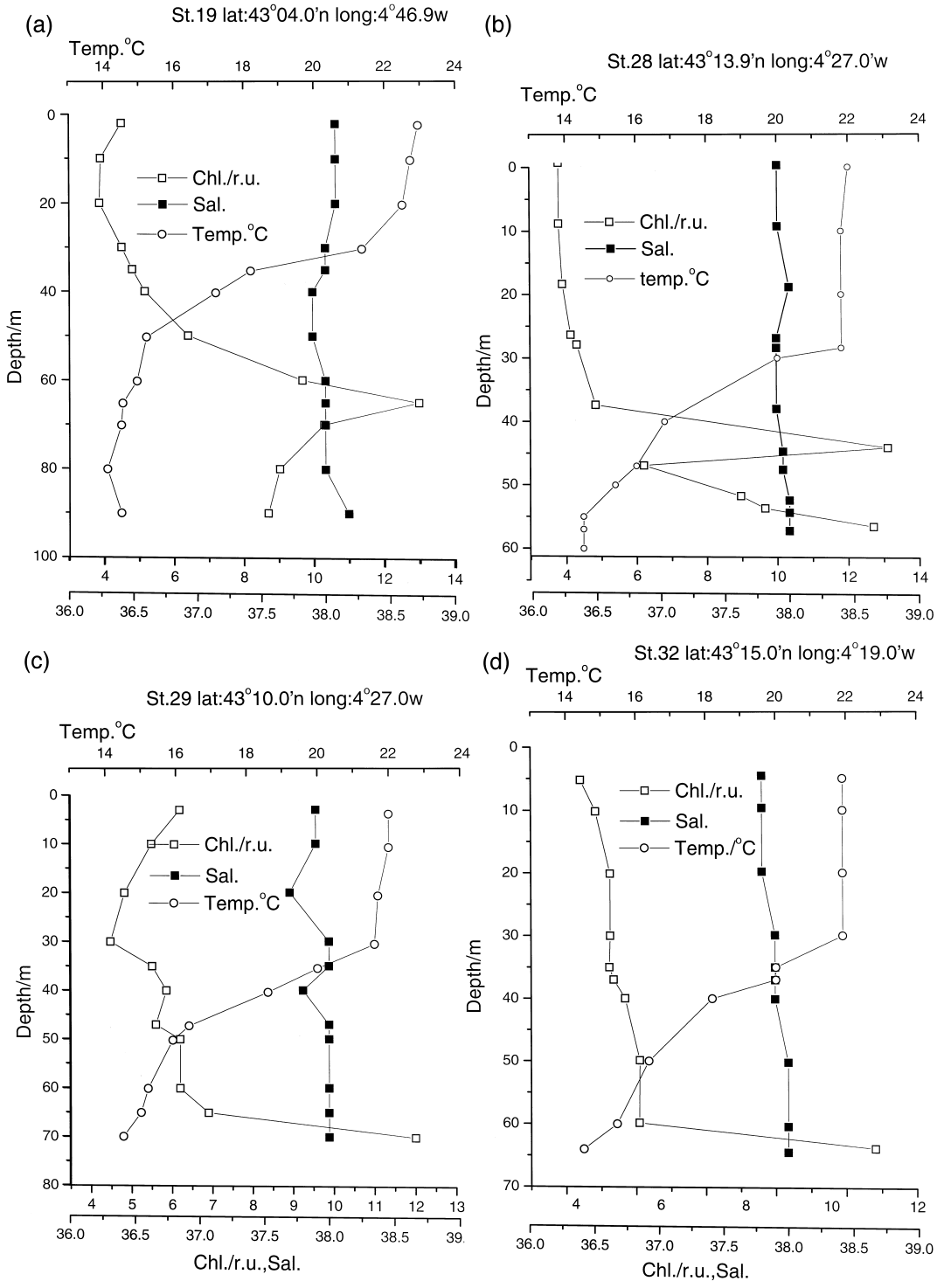

Fig. 3. (a,b,c,d) Multi-parametric vertical profiles (chlorophyll is expressed in relative units) of Stations 19, 28, 29, and 32 of the *Thetys* cruise in the Gulf of Lions (September–October 1997).

Stations 19, 28, 29, and 32, in the Gulf of Lions, vertical profiles of chlorophyll, temperature and salinity as evidence of the sharp stratification of the water masses. In the surface, the aCDOM slopes S are presumably affected by the Rhône river plume: 0.0178 ± 0.0029 for 17 stations in proximity of the river mouth, surprisingly similar to those found in surface blue waters: 0.0172 ± 0.003 for 15 stations. The waters below the thermocline are characterised by an average $S = 0.019 \pm 0.003$ for 27 observations and a Q.Y. $= 1.00$ (± 0.3) slightly higher than that found in surface which is equal to 0.96 (± 0.24). In this case, the probable photolysis effect can be masked by the differences existing in CDOM and in Q.Y. among the waters separated by the thermocline. In addition to the Rhône river inflow, into the Gulf of Lions, the hydrodynamics are also controlled by the cyclonic Ligurian current whose strength can induce the upwelling of deep water along the continental shelf (Beckers et al., 1997).

5.1. CDOM fluorescence and absorption relationship

The good correlation between fluorescence emission and absorption coefficient of CDOM at the wavelength used for the fluorescence excitation is now widely recognised despite the variability of the Q.Y. (Hoge et al., 1993; Green and Blough, 1994). The statistical expressions are given in Table 1, while Figs. 4a,b and 5a,b illustrate the relationship between aCDOM and fluorescence (St.F.U.) for the two measurement campaigns described here. These good relationships allow the inference of the CDOM absorption coefficient from the fluorescence emission signal using airborne Lidar system over large marine areas (Hoge et al., 1995a,b). The results of the relationships confirm those reported in the literature (Vodacek et al., 1995) although the direct comparison between the coefficients of the equations listed in Table 1 cannot be made because of the diverse methods of acquisition of the fluorescence

Table 1
Regression equations with the statistical parameters for the stations/samples of the cruises here described. Data from South Baltic Sea (1994) are added as comparison

Subset description	Month, year	No. of samples	Regression equations	Corr. coefficient r
South Baltic Sea[a]	April 1994	121	aCDOM(355) = 0.32($\pm$0.03) + 0.113($\pm$0.01)St.F.U.(355)	0.99
Gulf of Lions	Sept. 1997	78	aCDOM(355) = 0.028($\pm$0.017) + 0.174($\pm$0.01)St.F.U.(355)	0.89
Gulf of Lions[b]	Sept. 1997	58	aCDOM(355) = 0.037($\pm$0.013) + 0.135($\pm$0.011)St.F.U.(355)	0.84
N. Sea and Atlantic area	April 1997	66	aCDOM(355) = 0.015($\pm$0.0066) + 0.138($\pm$0.0031)St.F.U.(355)	0.98
Atlantic area	April 1997	54	aCDOM(355) = 0.0036($\pm$0.0096) + 0.099($\pm$0.013)St.F.U.(355)	0.71
Rhine r. Pl.	April 1997	11	aCDOM(355) = $-$1.067($\pm$0.78) + 0.003($\pm$0.01)DOC(μMC)	0.62
N. Sea and Atlantic area[b]	April 1997	43	aCDOM(355) = 0.028($\pm$0.0007) + 0.00036($\pm$0.000066)DOC(μMC)	0.66
South Baltic Sea[a]	April 1994	92	aCDOM(355) = $-$ 5.5($\pm$0.08) + 0.015($\pm$0.00047)DOC(μMC)	0.9
Rhône r. Pl. surface	Sept. 1997	19	St.F.U. = $-$2.09($\pm$1.45) + 0.023($\pm$0.007)DOC(μMC)	0.65
Gulf of Lions Chl max.depth[b]	Sept. 1997	20	St.F.U. = 0.15($\pm$0.21) + 0.0047($\pm$0.0015)DOC(μMC)	0.56
Gulf of Lions surface[b]	Sept. 1997	15	St.F.U. = 0.054($\pm$0.15) + 0.004($\pm$0.0018)DOC(μMC)	0.73

[a] Data from Ferrari et al. (1996).
[b] Data excluding the rivers plume.

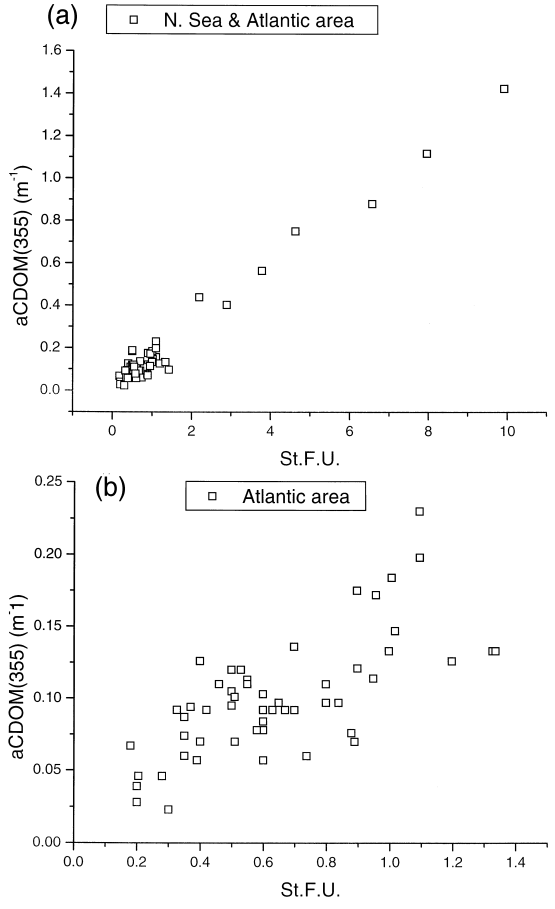

Fig. 4. (a and b) Relationship between absorption (at 355 nm in m^{-1}) and induced fluorescence (St.F.U. excitation wavelength = 355 nm, see in the text). The data refer to the *Victor Hensen* cruise for all the stations (a) and for the Atlantic area only (b). The statistical coefficients are given in Table 1.

units (Ferrari and Dowell, 1998). The linear equations presented above show that the slopes are similar for the stations collected in the Gulf of Lions, excluding the Rhône river plume, to those of European Atlantic areas including the river Rhine plume in the North Sea. This slope is only slightly different to that found in the South Baltic Sea (April 1994, Ferrari et al., 1996).

5.2. DOC and dissolved inorganic carbon (DIC)

Particular care has been dedicated to the sample preservation and to the HTCO–DOC analysis. With the awareness to have artifactual values due the chemical lability of DOM in aqueous solution, particular attention has been paid on: (1) reduction of the time between the sample collection and the analysis (maximum 3 weeks); (2) preservation temperature at 3°C in refrigerator; and (3) acidification with H_3PO_4 to reduce the bacterial activity. The bottles were filled to the top to minimise the volume of air in contact with the liquid surface to avoid oxidation. Blanks of campaign (bottle filled with Milli-Q water and acidified), per each 10 samples, were prepared and treated as the samples. This blank accounts for all the possible sources of spurious environmental contamination during the sample operations, and it has been measured on average as 25 μMC and then subtracted by each DOC measurement. The compre-

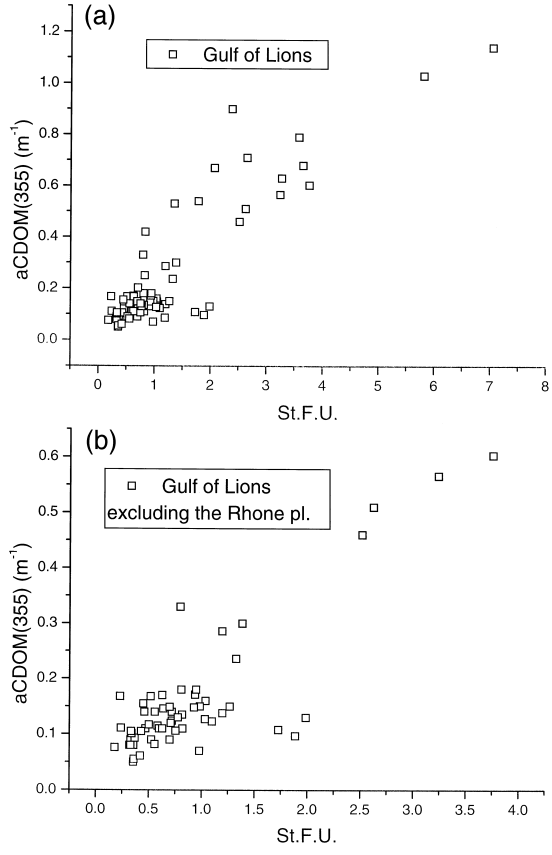

Fig. 5. (a and b) The same as Fig. 4, with the data refering to the *Thetys* cruise for all the stations (a) and excluding the Rhône river plume (b). The statistical coefficients are given in Table 1.

hensive data are reported in Appendices A and B. The average DOC levels measured in the Rhine river plume was found to be 542 ± 77 μMC, while in the surface, in the Rhône river tongue, was 331 ± 189 μMC. In the open sea (Atlantic), the average DOC level was 141 ± 76, while in deep waters (> 500 m) DOC was found to be 57 μMC, a value consistent with several literature data (Druffel et al., 1992; Sharp et al., 1995; Peltzer et al., 1996). In the Gulf of Lions, it is difficult to derive conclusions on DOC levels considering the distribution of the stations on the continental shelf inside and outside the Rhône river tongue. The samples, collected below the thermocline in deep waters at 14–15°C, gave a DOC concentration $= 130 \pm 45$ μMC while, in the real blue waters (Stations 25, 30, 33, 34 and 35), we have found 109 ± 31 in the surface and 90 ± 35 in the depth, data consistent with those reported by Cauwet et al. (1997). Some interesting results were acquired from the relationship between DOC and CDOM absorption and fluorescence. Table 1 summarises the statistical relationship between aCDOM at 355 nm as well as St.F.U. and DOC. The data set was subdivided to study separately the Rhine river and Rhône river plumes. Actually, from these fits it is evident that a large fraction of DOC that is non-absorbing of visible light resides in DOM. Considering as valid the statistical coefficient listed in Table 1, the non-absorbing DOC appears to be 50–60% for the Rhine plume, and 45% for the Rhone plume, where the fluorescence was found better related to DOC. The percentages were obtained on the total DOC values on average. The data, outside the river plumes, suggests the following considerations: (1) the slopes of the best fit are lower with respect to the data considered as whole and (2) if the linear fit is logically used, no intercept can be drawn, indicating that all the DOM exhibits chromophoric properties. Consequently, aCDOM correlates with the DOC at low concentration. If this is true, as it seems at least for the data considered, aCDOM can act as a tracer for DOM pools outside the continental influences. Fig. 6 shows the statistical dependency of aCDOM on DOC for the Atlantic and North Sea areas including Rhine river plume. Fig. 7 illustrates the relationships between St.F.U. and DOC for the Gulf of Lions, showing the Rhône plume and the rest of the stations in surface and in depth.

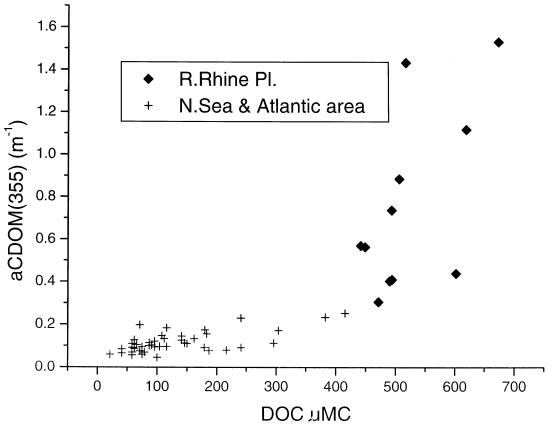

Fig. 6. Relationship between aCDOM and DOC for all the stations of the *Victor Hensen* cruise. The statistical coefficients are given in Table 1.

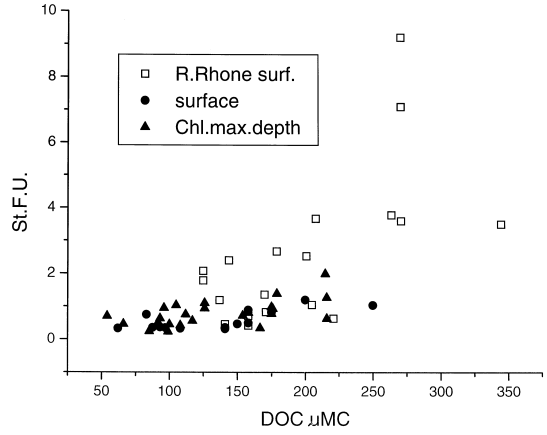

Fig. 7. Relationship between St.F.U. and DOC. The statistical coefficients are given in Table 1.

DIC, which represents the DOC fraction mineralised to CO_2, has been estimated for the stations of the Gulf of Lions characterised by a stable water-stratified situation. The stations that have been chosen are not directly affected by the river Rhône fresh waters as well as by the deep-water upwelling. The expression used was the following (Vodacek et al., 1997):

$$\mathrm{fDIC} = (1 - \mathrm{fDOC})/(1 - a_F/a_I) \quad (5)$$

with $\mathrm{fDOC} = [\mathrm{DOC}_F]/[\mathrm{DOC}_I]$

Table 2
Stations' (*Thetys* cruise) basic data and final calculations of the fraction of DOC mineralized to CO_2

Station (depth)	aCDOM (350)	DOC (μMC)	1 − fDOC	$1-(a_F/a_I)$	fDIC	fDIC[a]
19/00	0.074	158	0.048	0.699	0.0686	0.104
19/65	0.246	166				
32/00	0.138	92	0.0416	0.496	0.084	0.074
32/65	0.274	96				
31/00	0.094	93	0.07	0.447	0.156	0.067
31/15	0.17	100				
34/00	0.061	87	0.0645	0.435	0.148	0.065
34/60	0.108	93				
28/00	0.11	108	0.0645	0.251	0.258	0.037
28/55	0.147	127				
29/00	0.087	97	0.1638	0.514	0.318	0.076
29/70	0.179	116				

[a]Values calculated using the Miller and Zepp (1995) formula.

where, fDIC is the fraction of the initial DOC mineralised to CO_2 divided by the fraction of aCDOM at 350 nm in the surface layer (F as final, after the photo-oxidation) with respect to the aCDOM at 350 nm in the layer immediately below (I as initial, not affected by the photo-oxidation). The same subscripts F and I are used for [DOC] concentration. Further, for the same stations, DIC has been calculated with the Miller and Zepp (1995) formula and the results compared with our values. In Stations 19, 31, 32, and 34, a possible influence of the deep water (upwelling) can be excluded. Here the fDIC values 0.068, 0.156, 0.08, and 0.148, respectively, are similar, or slightly higher, to those calculated using the slope 0.149 (as in Miller and Zepp, 1995) obtained by a laboratory photo-oxidation experiment using natural CDOM rich waters: 0.1, 0.07, 0.074, and 0.065. The result of this comparison demonstrates an effective DOC photo-mineralization with DIC production. An experiment of DIC measurement with sequential bacterial (dark incubation) and photochemical degradation on humic substance concentrates has been performed by Miller and Moran (1997). This combination of bacterial and photochemical degradation resulted in 8–13% losses of DOC consistent with our finding of fDIC which is on average 11%. In the stations 28 and 29, where the underlying layers can be probably upwelling dominated, the difference in fDIC are more marked: 0.258 and 0.318 with respect to 0.037 and 0.076 obtained with the Miller and Zepp formula. In this case, the differences in aCDOM and DOC among the two adjacent water layers are, in addition to the photo-oxidation effect, mostly due to the high CDOM and DOC concentrations of the bottom water along the continental margin of Gulf of Lions. All the data of this computation are listed in Table 2 and the station

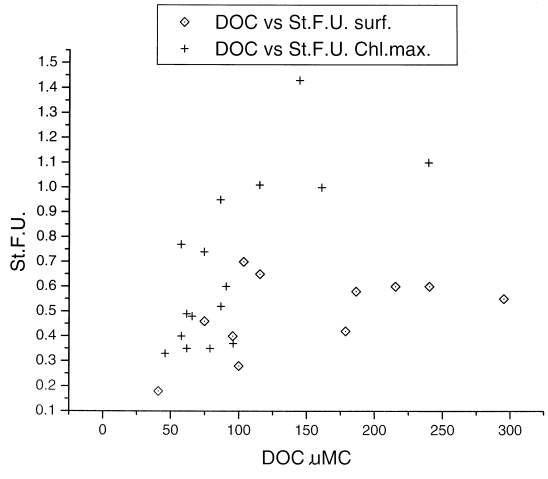

Fig. 8. Relationship between St.F.U. and DOC of oceanic/open-sea stations (*Victor Hensen* cruise) where the fluorescence has been measured. The figure shows data collected in surface compared to those at the chlorophyll maximum depth. The specific DOC fluorescence is on average higher in depth than in surface as evidence a possible photo-alteration effect.

locations in Table 1. Further, multi-parametrical profiles of four among the six stations here considered are illustrated in Fig. 3.

The photo-bleaching effect appears more evident using fluorescence than absorption because it is a more sensitive signal as shown in Fig. 8 for open sea stations of the *Victor Hensen* cruise.

5.3. Quantum yield

As already stated in previous paragraphs, quantum yield differences do not prevent the good correlation between CDOM absorption and fluorescence. The averaged values found are 0.91 and 0.96 in the surface waters in the Rhine river and Rhône river plumes, respectively. The values are slightly higher at the euphotic depth: 0.99 and 1.00, but they become higher below the euphotic depth and namely in the cold upper Mediterranean waters (upwelling) as well as in the deep waters of the Atlantic at the summit of the sea mounts: 1.18 and 1.06, respectively.

6. Conclusions

The results presented in this work lead to the following conclusions.

(a) The good relationship between CDOM absorption coefficient and fluorescence, despite the Q.Y. variations, has became a solid achievement. The present results show that, if the data of the Rhine plume is excluded, the statistical coefficients are similar despite the different study sites and different seasons (European Atlantic areas in April and Mediterranean area in September–October). These particular optical properties of CDOM allow the inference of absorption coefficient from fluorescence measured by a Lidar system over large areas.

(b) CDOM absorption coefficient has been found correlated with DOC in the North Sea and Atlantic area whereas only the fluorescence (St.F.U.) has been found correlated with DOC in Mediterranean area (Gulf of Lions). In the river plumes, (Rhine and Rhône) a large amount of DOC belongs to the portion of the DOM pool that is non-absorbing in visible light. At the other sites, the linear regression found do not display an intercept, demonstrating that all the DOM is chromophoric. The small slope (0.00036 vs. 0.015 found in South Baltic Sea, in Table 1) indicates a low DOC specific absorption in the DOM pool. The same conclusion can be derived for the Gulf of Lions (excluding the Rhone plume) with the use of fluorescence instead aCDOM. In the river plume areas, the slopes are 5–10 times greater than in the open sea without fluvial influence. The relationship presented here, in addition to those found in other marine areas such as the Baltic Sea (Ferrari et al., 1996) and in the U.S. Atlantic coasts (Vodacek et al., 1997), are not applicable to other sites and even, at the same site, to other seasons. However, they represent an important tool in support of local studies of carbon fluxes using remote sensing techniques. These can be active, through the already cited airborne Lidar systems, or passive when the algorithms, whose studies are in progress, will be able, thanks to the new and the future sensors (MERIS, MODIS, ADEOS) [1], to detect CDOM in an independent way from the suspended sediment and the photosynthetic pigments.

Acknowledgements

The field work was carried out on board R/V *Victor Hensen* and *Thetys* during two measurement cruises organised in the framework of the CoastLooc project funded by the European Commission. I express my gratitude to the respective captains and the crew for their collaboration. I wish to acknowledge the valuable collaboration work made by Mr. Franco Bo (Environment Institute of JRC Ispra), for the DOC analyses. I thank Dr. Hans Barth (university of Oldenburg, Germany) for providing the CTD profiles. I thank also Grigor Obolensky, Brian Hosgood and Mark Dowell for the editing of the manuscript. This work has benefited from very thorough criticisms and suggestions of two anonymous referees.

[1] MERIS: Medium Resolution Imaging Spectrometer; MODIS: Moderate Resolution Imaging Spectrometer; ADEOS: Advanced Earth Observing Satellite.

Appendix A. List of the stations and data of the *Victor Hensen* cruise

a355 is the CDOM absorption coefficient at 355 nm (m^{-1}) and S is the spectral slope of Eq. 1. Quantum Yield (Q.Y.) is calculated with Eq. 4 while DOC, expressed in micro-moles of C, is analysed with HTCO method, and the salinity is obtained with the CTD. The empty spaces are missing data while n.m. corresponds to non-measurable value.

Station no.	Depth, m	a350, m^{-1}	S, nm^{-1}	Q.Y., %	DOC, μMC	Salinity
VH01	0	0.32	0.0165		605	35
VH02	0	0.289	0.0208	1.54	663	35
VH03	0		0.0189		495	35
VH04	0	0.439	0.0288		472	35
VH05	0	0.564	0.0176	0.76	603	34.9
VH06	0	0.616	0.0182	1.19	450	34
VH06	16	0.403	0.0223	1.05	491	34
VH07	0	1.117	0.0206	1.05	622	33
VH07	17	0.57	0.022		443	34
VH08	0	1.53	0.0177		677	27
VH08	18	0.737	0.0195	0.91	495	33
VH09	0	1.423	0.0191	1.02	520	25
VH09	17	0.885	0.0212	1.16	508	33
VH10	0		0.0202		416	24.9
VH10	30		n.m.		383	33
VH11	0	0.156	0.0193	0.76	183	35.5
VH11	20	0.133	0.018		112	35.5
VH11	60	0.175	0.023		180	35.5
VH12	0	0.126	0.0157	0.96	95.7	35.7
VH12	80	0.121	0.022	0.99		35.7
VH13	0	0.0966	n.m.	1.05	104	35.7
VH13	150	0.154	0.014	0.76	116	35.7
VH14	0	0.1127	0.0301	0.76		35.7
VH14	150	0.184	0.018	0.99	108	35.7
VH14	260	0.11	0.0155	0.61	150	35.7
VH15	0	0.0966	0.0172	0.99	116	35.7
VH15	180	0.133	0.0176	1.05	162	35.7
VH15	360	0.172	0.015	0.82	304	35.7
VH16	0	0.096	0.029	1.16	75	35.7
VH16	100	0.126	0.019	1.28	141	35.7
VH16	250	0.145	n.m.	1.4	141	35.7
VH17	0	0.078	0.032	1.05	187	35.7
VH18	0	0.08	n.m.	1.19	216	35.7
VH18	50	0.113	0.019	2.19	146	35.7
VH18	100	0.23	0.013	0.67	241	35.7
VH19	0	0.092	n.m.	0.93		35.9
VH19	30	0.103	0.02	0.82	91	35.9
VH19	75	0.11	0.013	0.61	58	35.9
VH19	100	0.105	0.011	0.6	66	35.9
VH19	1080	0.092	0.011	1.05	58	35.9

Station no.	Depth, m	a350, m^{-1}	*S*, nm^{-1}	Q.Y., %	DOC, μMC	Salinity
VH20	0	0.198	0.011	0.9	71	35.8
VH20	50	0.07	0.012	1.02	79	35.8
VH20	100	0.07	0.013	0.96	58	
VH21	0		0.012		75	35.9
VH21	50	0.127	0.014		62	35.9
VH22	0	0.093	0.024	0.64	179	
VH22	80	0.101	0.011	0.88	87	
VH23	0	0.074	0.015	0.88		
VH23	33	0.06	n.m.		75	
VH23	200	0.057			58	
VH23	790	0.076			71	
VH24	0	0.046	0.013	0.81	100	36.7
VH24	100	0.094	0.014	1.08	96	36.5
VH24	1020	0.085	0.009	0.85	41	
VH25	0	0.046	n.m.	0.64		36.6
VH25	75	0.087	0.017	0.58	62	36.4
VH25	690	0.11	0.0106	0.76		35.5
VH26	0	0.0667	0.017	0.4	41	36.5
VH26	40	0.092	n.m.	0.52	46	36.5
VH27	0	0.04	0.017	0.7		36.7
VH27	50	0.114	0.023	1.34	87	36.6
VH27	150	0.078	0.0096	1.19	58	36.2
VH27	920	0.07	n.m.		58	
VH28	0	0.028	n.m.			36.8
VH28	100	0.06	n.m.		21	36.8
VH29	0	0.023	n.m.			36.5
VH29	87	0.057	n.m.			36.5
VH30	100	0.108	n.m.	0.44		36.8
VH30	200	0.16	0.0128	0.55		36.2
VH30	700	0.052	n.m.			
VH32	0	0.083	0.014			36.7
VH32	800	0.092	0.014			
VH33	0	0.044	n.m.			36.7
VH33	102	0.09	0.017			36.7
VH33	200	0.07	0.025			36.45
VH33	800	0.062	n.m.			
VH34	0	0.027	n.m.			36.7
VH34	75	0.108	n.m.	0.38		36.5
VH34	200	0.05	n.m.	1.45		36.2
VH34	750	0.069	n.m.	1.51		
VH35	0	0.092	0.016	0.61		36.7
VH35	71	0.071	n.m.	0.79		36.7
VH35	150	0.064	0.018	1.02		36.4
VH36	0	0.126	0.0146			36.7
VH36	83	0.126	0.0148			36.7
VH36	150	0.119	0.011			36.4
VH37	82	0.23	0.011			36.7

Station no.	Depth, m	a350, m^{-1}	*S*, nm^{-1}	Q.Y., %	DOC, μMC	Salinity
VH37	151	0.037	n.m.			36.3
VH38	0	0.041	n.m.			36.7
VH38	82	0.21	0.011			36.75
VH38	1200	0.066	n.m.			
VH39	0	0.13	0.014			36.68
VH39	80	0.35	0.011			36.7
VH40	0	0.1	0.021			36.7
VH40	90	0.17	0.0106			36.5
VH41	0	0.097	0.018			36.75
VH41	100	0.218	0.012			36.55
VH42	0	0.079	0.014			36.75
VH42	70	0.083	n.m.			36.7
VH43	0	0.057	0.016			36.8
VH43	83	0.13	0.013			36.8
VH44	0	0.103	0.012			36.8
VH44	75	0.103	0.018			36.8
VH45	60	0.035	n.m.			36.8
VH46	0		n.m.		10	36.8
VH46	50	0.069	n.m.		62	36.8

Appendix B. List of the stations and data of the *Thetys* cruise

Abbreviations are the same as in Appendix A.

Sample no.	Depth, m	a350, m^{-1}	*S*, nm^{-1}	Q.Y., %	DOC, μMC	Salinity
The01	0	0.148	n.m.	1.3	206	
The02	0	0.289	0.0145	0.92	200	36
The02	25	0.33	0.0167	0.54	275	38
The03	0	0.11	n.m.	1.67	175	38
The03	65	0.13	0.022		215	37.8
The04	0	0.16	0.024	1.3	250	37
The04	60	0.296	0.0145	0.99	179	38
The05	0	0.13	0.017	1.3	291	37.5
The05	60	0.16	0.027	1.1	346	37.9
The07	0	0.42	0.013	0.46	396	
The07	30	0.168	0.021	0.63		
The08	0	0.52	0.0166	0.57		36.3
The08	30	0.11	0.0168	0.53	83.3	38.1
The08	45	0.537	0.0165		125	37.9
The09	0	0.9	0.0166	0.6	141	34
The09	25	0.14	0.0155	0.7	154	38.2
The10	0	0.71	0.017	0.89	146	37.5
The10	4	0.1	0.019		121	37.5
The10	20		0.017	0.75		38.1
The10	60	0.14	0.027		112	38
The11	0	0.117	n.m.	0.97	150	

Sample no.	Depth, m	a350, m^{-1}	*S*, nm^{-1}	Q.Y., %	DOC, μMC	Salinity
The11	60			1.1	175	
The12	0	0.117	0.013	1.04	158	38
The12	70	0.146	0.016	1.07	67	38
The13	0	0.126	0.0177			38.1
The13	60	0.17	0.022			38
The14	0	0.54	0.016	0.72	125	33.5
The14	20	0.097	0.028		71	38
The15	0	0.67	0.015	0.7	125	35.5
The15	50	0.14		0.71	66	38
The16	0	0.68	0.022	1.22	208	36
The17	0	0.79	0.0162	1.01	271	38
The17	70	0.17	0.0172	0.89	216	38
The18	0	0.25	0.0174	0.75	171	37.3
The18	70	0.15	0.0184	1.86	216	38
The19	0	0.07	0.011		158	38
The19	60	0.18	0.019	1	166	38
The20	0	0.103	n.m.	0.92	158	37.9
The21	0	0.12	0.0175	0.83	141	37
The21	30	0.09	0.018		241	38.1
The22	0	0.168	0.017	0.81	221	36
The22	40	0.11	n.m.	1.22	158	38
The23	0	0.202	0.0183	0.75	158	35.2
The23	30	0.137	0.0167			38
The23	60	0.124	n.m.	1.22	154	38
The24	0	0.181	0.021		204	35.2
The24	60	0.156	0.018		229	38
The25	0	0.076	n.m.	0.85	117	38
The25	65	0.168	0.016	1.05	100	38
The26	0	0.085	n.m.		137	38
The27	0	0.085	n.m.	2.07	126	38
The27	35	0.148	0.022	1.2	177	37.7
The28	0	0.09	0.0174	0.7	108	37.8
The28	55	0.171	n.m.	1.04	127	38
The29	0	0.08	n.m.	0.84	97	38
The29	60	0.14	0.02	0.7	116	38
The30	0	0.08	0.021	0.75	142	38
The30	70	0.149	n.m.	0.92	54	37.8
The31	0	0.093	n.m.	0.77	93	37.5
The31	15	0.155	0.015	0.57	100	37.5
The32	0	0.105	0.0177	0.81	92	37.6
The32	65	0.18	0.0201	0.98	96	38
The33	0	0.08	0.0184	0.75	62	38
The33	40	0.102	n.m.	0.62		37.8
The33	70	0.12	n.m.		93	38
The34	0	0.05	n.m.	1.38	87	38.1
The34	60	0.11	n.m.	1.07	93	38
The35	0	0.055	n.m.	1.27	141	38.1

Sample no.	Depth, m	a350, m^{-1}	*S*, nm^{-1}	Q.Y., %	DOC, μMC	Salinity
The35	84	0.106	n.m.	1.3	112	38.2
The36	0	0.566	0.018	1.11	181	37.5
The37	0	0.604	0.0178	1.18	264	34.9
The37	50	0.061	n.m.	1.35	108	38
The38	0	0.46	0.0156	1.06	202	35
The38	82	0.135	n.m.	1.1	112	38
The39	0	0.51	0.0159	0.98	179	35
The39	70	0.13		1.16	175	38
The40	0	0.14	0.02	1	83	38
The40	89	0.127	0.021	1.57	104	38
The41	0	0.09	0.0134	1.05	162	
The42	0	0.105	n.m.	0.64	158	
The44	0	0.083	n.m.	1.26		
The44	53	0.108	n.m.			
The45	0	1.14	0.017	1.11	271	
The45	73	0.236	0.016	1		
The46	0	1.03	0.016	1.02		
The47	0	0.62	0.016	0.96	346	
The48	0	1.71	0.0258	0.98	271	

References

Bacastow, R., Maier-Reimer, E., 1991. Dissolved organic carbon in modelling oceanic new production. Global Biogeochem. Cycles 5, 71–85.

Beckers, J.M., Brasseur, P., Nihoul, C.J., 1997. Circulation of the western Mediterranean: from global to regional scales. Deep-Sea Res. II 44 (3–4), 531–549.

Bricaud, A., Morel, A., Prieur, L., 1981. Absorption by dissolved organic matter of the sea (yellow substance) in the UV and visible domains. Limnol. Oceanogr. 26, 43–53.

Brugger, A., Slezak, D., Obernosterer, I., Herndl, G.J., 1998. Photolysis of dimethylsulfide in the northern Adriatic Sea; Dependence on substrate concentration, irradiance and DOC concentration. Mar. Chem. 59, 321–331.

Cauwet, G., 1994. HTCO method for dissolved organic carbon analysis in sea-water: influence of catalyst on blank estimation. Mar. Chem. 47, 55–64.

Cauwet, G., Miller, A., Brasse, S., Fengler, G., Mantoura, R.T.C., Spitzy, A., 1997. Dissolved and particulate organic carbon in the western Mediterranean Sea. Deep-Sea Res. 44 (3–4), 769–779.

Chen, R.F., 1999. In situ fluorescence measurements in coastal waters. Org. Geochem. 30, 397–409.

Druffel, E.M., Williams, P.M., Bauer, J.E., Ertel, J.R., 1992. Cycling of dissolved and particulate organic matter in the open ocean. J. Geophys. Res. 97, 15639–15659.

Ferrari, G.M., Dowell, D., 1998. CDOM absorption characteristics with relation to fluorescence and salinity in coastal areas of the southern Baltic Sea. Est. Coast. Shelf Sci. 47, 91–105.

Ferrari, G.M., Tassan, S., 1991. On the accuracy of determining the light absorption by ''yellow substance'' through measurement of induced fluorescence. Limnol. Oceanogr. 36, 777–786.

Ferrari, G.M., Dowell, M.D., Grossi, S., Targa, C.C., 1996. Relationship between the optical properties of chromophoric dissolved organic matter and total concentration of dissolved organic carbon in the southern Baltic Sea region. Mar. Chem. 55, 299–316.

Green, S.A., 1992. Application of fluorescence spectroscopy to environmental chemistry, Ph.D. Thesis, Massachusetts Institute of Technology/Woods Hole Oceanography Institution, Woods Hole, MA, Joint Progr. Oceanogr.

Green, S.A., Blough, N.V., 1994. Optical absorption and fluorescence properties of chromophoric dissolved organic matter in natural waters. Limnol. Oceanogr. 38, 1903–1916.

Helz, G.R., Zepp, R.G., Crosby, D.G. (Eds.), Aquatic and Surface Photochemistry. Lewis Publisher, Boca Raton, FL.

Heuermann, R., Loquay, K.D., Reuter, R., 1995. A multi-wavelength ''in situ'' fluorometer for hydrographic measurements. In: EARSeL Adv. In Remote Sensing. p. 3.

Hoge, F.E., Vodacek, A., N.V. Blough, N.V., 1993. Inherent optical properties of the ocean: retrieval of the absorption coefficient of chromophoric dissolved organic matter from fluorescence measurements. Limnol. Oceanogr. 38, 1394–1402.

Hoge, F.E., Williams, M.E., Swift, R.N., Yungel, J.K., Vodacek, A., 1995a. Satellite retrieval of the absorption coefficient of chromophoric dissolved organic matter in continental margins. J. Geophys. Res. 100, 24847–24854.

Hoge, F.E., Vodacek, A., Swift, R.N., Yungel, J.K., Blough,

N.V., 1995b. Inherent optical properties of the ocean: Retrieval of the absorption coefficient of chromophoric dissolved organic matter from airborne laser spectral fluorescence measurements. Appl. Opt. 34 (30), 7033–7038.

Højerslev, N.K., 1988. In: Natural Occurrences and Optical Effects of Gelbstoff, Copenhagen University Rep. 50, 30 pp.

Jackson, A.G., 1993. The importance of the DOC pool for primary production estimates. ICES Mar. Sci. Symp. 197, 141–148.

Miller, W.L., Moran, M.A., 1997. Interaction of photochemical and microbial processes in the degradation of refractory dissolved organic matter from a coastal marine environment. Limnol. Oceanogr. 42 (6), 1317–1324.

Miller, W.L., Zepp, R.G., 1995. Photochemical production of dissolved inorganic carbon from terrestrial organic matter: Significance to the oceanic organic carbon cycle. Geophys. Res. Lett. 22 (4), 417–420.

Naudin, J.J., Cauwet, G., Chretiennot-Dinet, M.J., Deniaux, B., Devenou, J.L., Pauc, H., 1997. River discharges and wind influence upon particulate transfer at the land-ocean interaction. Case study of the Rhône River plume. Est. Coast. Shelf Sci. 45, 303–316.

Nieke, B., Reuter, R., Heuermann, R., Wang, H., Babin, M., Therriault, J.C., 1997. Light absorption and fluorescence properties of chromophoric dissolved organic matter (CDOM), in the St. Lawrence Estuary (Case 2 waters). Cont. Shelf Res. 17, 235–252.

Peltzer, T.E., Fry, B., Doering, P.H., McKenna, J.H., Norrmann, B., Zweifel, U.L., 1996. A comparision of methods for the measurement of dissolved organic carbon in natural waters. Mar. Chem. 54, 85–96.

Sharp, J.H., 1997. Marine dissolved organic carbon, Are the older values correct? Mar. Chem. 56, 265–277.

Sharp, J.H., Benner, R., Bennet, L., Carlson, C.A., Fitzwater, S.E., Peltzer, E.T., Tupas, M., 1995. Analyses of dissolved organic carbon in seawater: the JGOFS EqPac. methods comparison. Mar. Chem. 48, 91–108.

Vodacek, A., Hoge, F.E., Swift, R.N., Yungel, J.K., Peltzer, E.T., Blough, N.V., 1995. The in situ and airborne fluorescence measurements to determine UV absorption coefficients and DOC concentrations in surface waters. Limnol. Oceanogr. 40, 411–415.

Vodacek, A., Blough, N.V., DeGrandpre, M.D., Peltzer, E.T., Nelson, R.K., 1997. Seasonal variation of CDOM and DOC in the Middle Atlantic Bight: terrestrial inputs and photo-oxidation. Limnol. Oceanogr. 42 (4), 674–686.

Zepp, R.G., Wolfe, N.L., Baughman, G.L., Hollis, R.C., 1977. Singlet oxigen in natural waters. Nature 267, 421–423.